Colloid Polym Sci 280: 245–253 (2002)

ORIGINAL CONTRIBUTION

Szabolcs Vass
Kristina Haimer
Gerhard Meier
Markus Klapper
Sándor Borbély

Small-angle neutron scattering study of poly(methyl methacrylate-*block*-sodium acrylate-*block*-methyl methacrylate) and poly(sodium acrylate-*block*-methyl methacrylate-*block*-sodium acrylate) triblock copolymers in aqueous solutions

Received: 20 December 2000
Accepted: 18 August 2001

S. Vass (✉)
KFKI Atomic Energy Research Institute
P.O. Box 49, 1525 Budapest, Hungary
e-mail: szvass@sunserv.kfki.hu
Tel.: +36-1-3922222, ext. 3632
Fax: +36-1-3922299

K. Haimer · G. Meier · M. Klapper
Max Planck Institute for Polymer Research, 10 Ackermannweg
55128 Mainz, Germany

G. Meier
Institute for Solid State Research
Research Center Jülich
52425 Jülich, Germany

S. Borbély
Research Institute for Solid State Physics and Optics
P.O. Box 49, 1525 Budapest, Hungary

Abstract Small-angle neutron scattering experiments were made on poly(methyl methacrylate-*block*-sodium acrylate-*block*-methyl methacrylate) [p(MMA-*b*-NaA-*b*-MMA)] and p(NaA-*b*-MMA-*b*-NaA) solutions by varying the composition and the concentration of the polymer with and without 1 M NaCl added. Scattering curves could be evaluated by assuming that the polymers aggregate into polydisperse micelles. The experiments support the expectation that in the case of the p(MMA-*b*-NaA-*b*-MMA) block sequence the hydrophilic blocks form closed loops connected by both ends to the micellar cores; in the case of the p(NaA-*b*-MMA-*b*-NaA) block sequence they float freely in the solvent. The micellar cores exert considerable stability against dilution and added electrolyte. The interaction of charged micelles could be formally described in terms of volume exclusion and the Derjaguin–Landau–Verwey–Overbeek potential.

Keywords Small-angle scattering · Ionic triblock copolymers (ABA and BAB) · Derjaguin–Landau–Verwey–Overbeek theory

Introduction

In recent years, block copolymers have gained increasing importance as stabilizers in emulsion polymerization owing to their many advantages over conventional low-molecular-weight surfactants. The parameters of the end product can be influenced by the choice of the emulgator in the polymerization and stabilization phases. In the polymerization phase the basic process is the solubilization of monomers by emulgator micelles, which may be influenced by the structure of the micelles and the hydrocarbon/water interface. Provided that the emulgator becomes part of the polymer, it can play a role in the stabilization phase in determining the interactions between the polymer particles. In the case of ionic emulgators the electrostatic component of the interactions among the polymer particles will presumably be similar to that acting among the emulgator micelles.

Though the main principles for applying emulsion polymerization technology are empirically well known, the details of the processes on the molecular level are still not completely understood, especially in the case of ionic emulgators. Such emulgators are the newly developed ionic triblock copolymers [1, 2], built up of hydrophobic (A) poly(methyl methacrylate) (pMMA) and hydrophilic (B) poly(sodium acrylate) (pNaA) blocks, with both possible – ABA and BAB – block sequences. The block sequence allows various aggregation forms: one can expect unimolecular micelles, but also more complex structures, such as micelles consisting of closed loops, partly open or even cross-linked networks [3–6]. The aim of the present work is to decide by small-angle neutron

scattering (SANS) which type of aggregate is formed in aqueous (D_2O) solutions and to determine their most characteristic parameters.

An important problem related to small-angle scattering studies of ionic colloids is the representation of the interparticle interactions. On the basis of the similarity of ionic polymer and surfactant micelles, an attempt is made to describe the intermicellar interactions, at least empirically, with a combination of hard-sphere and Derjaguin–Landau–Verwey–Overbeek (DLVO) potentials [7]. The experiments with polymers of both ABA and BAB block sequences were done at room temperature, with different solute concentrations, with and without electrolyte added.

Materials and methods

The common way to synthesize triblock copolymers is anionic polymerization using difunctional initiators. Because of the enhanced sensitivity to impurities and side reactions leading to broad or bimodal molecular-weight distributions, only very few such initiator systems are known. Therefore, a new suitable difunctional initiator based on dihydroantrachene dimers had to be developed [1, 2] for producing triblock copolymers both with ABA and BAB sequences of the pMMA and pNaA blocks. This method ensures the control of the molecular weight and its distribution. The polymerization proceeds via a living mechanism, which allows successive addition of different monomers. Because neither NaA nor acrylic acid can be polymerized anionically, *t*-butyl acrylate has to be used instead. The hydrophilic blocks are introduced into the polymer by subsequent hydrolysis of the *t*-butyl ester groups to the acid, which can then be transformed into the sodium salt [2, 8, 9]. The composition and molar mass of the solutes are given in Table 1.

In the acid form, the polymers cannot be dissolved in water directly. First they must be predissolved in methanol, after which the poly(acrylic acid) is converted into the sodium salt by addition of an equivalent amount of dilute sodium hydroxide solution. Stock solutions of the copolymers were prepared by predissolving the samples under argon in hot deuterated methanol and adding one equivalent of NaOD (0.1 N in D_2O) as determined by potentiometric titration while still heating. After dilution with D_2O and heating the solution under argon for 30 min with a water bath at approximately 60 °C, methanol was removed by azeotropic distillation under reduced pressure. Gas chromatography tests indicated that the amount of residual methanol in the samples was negligible. The stock solutions had a concentration of several grams per liter; samples diluted by D_2O were poured into Hellma cuvettes of 5-mm pathlength.

SANS measurements were performed at the Budapest Neutron Center and at the Research Center Jülich with the KWS2 diffractometer. The mean neutron wavelength, $\bar{\lambda}$, was 0.346 and 0.79 nm, defined in both laboratories by helical slot selectors producing a nearly Gaussian wavelength distribution, $f_w(\lambda) = (1/\Delta\lambda\sqrt{2\pi})\exp[-(\lambda-\bar{\lambda})^2/(\sqrt{2}\Delta\lambda)^2]$ of relative spread, $\Delta\lambda/\bar{\lambda}$, ~13% and ~18%, respectively. Scattered neutrons were registered by ^{3}He gas detectors, built from a 64 × 64 array of 1 × 1-cm^2 pixels in Budapest and from the same array of 0.8 × 0.8-cm^2 pixels in Jülich. The Q ranges applied were 0.15–1.2/5 (in Budapest) and 0.04–1.2 nm^{-1} (in Jülich). The temperature was maintained within 0.5 K. The raw SANS patterns measured in Budapest and in Jülich were converted into absolute units using 1-mm thick H_2O and Lupolen standards, respectively. Because in one of the two experimental setups the slit geometry was circular and the other was quadratic, and the latter lacked even an approximate collimation correction procedure, the collimation correction of raw data has been omitted. Because the collimation correction affects the fit only in the vicinity of sharp peaks, its omission, according to our experience, may cause a change 3–5% or less in the best-fit values of the structural parameters.

Table 1 Composition of the triblock copolymers synthesized with polydispersity index (*PDI*) and molar mass (M_n). Methyl methacrylate (*MMA*), sodium acrylate (*NaA*)

Polymer	Type	Composition	PDI	M_n
P27	ABA	$(MMA)_{177}$–$(NaA)_{708}$–$(MMA)_{177}$	1.07	100,600
P32	ABA	$(MMA)_{65}$–$(NaA)_{260}$–$(MMA)_{65}$	1.12	37,500
P33	ABA	$(MMA)_{10}$–$(NaA)_{40}$–$(MMA)_{10}$	1.14	5,800
P8	BAB	$(NaA)_{90}$–$(MMA)_{90}$–$(NaA)_{90}$	1.20	25,600

Results and discussion

Results at higher Q

Polymers of ABA block sequence were fabricated at different times. The first load consisted of P27-, P32- and P33-type molecules, which were studied as a function of concentration at 298 K in Budapest; the results are plotted in Fig. 1. Owing to the relatively high Q values, no interaction peak can be observed in the scattering patterns.

The raw data suggest that the scattering intensity arises from homogeneous – and presumably polydisperse – spheres:

$$\frac{d\Sigma(Q)}{d\Omega} = n_{sc}(\Delta\rho)^2 \int_0^\infty F^2(Q,R) f_Z(R) dR \ , \qquad (1)$$

where n_{sc} is the number of scatterers per unit volume, $\Delta\rho$ is the scattering contrast and $F(Q, R) = 4\pi[\sin(QR) - QR\cos(QR)]/Q^3$ is the scattering amplitude of a homogeneous sphere of radius R and of unit scattering contrast. Finally, $f_Z(R) = \gamma(Z+1)(R/\bar{R})^Z \exp[-(Z+1)R/\bar{R}]$ is the Schulz–Zimm distribution function, $\gamma(Z+1) = (Z+1)^{Z+1}/\Gamma(Z+1)$, and $\Gamma(Z+1)$ is the gamma function; $\bar{R}$ equals the mean value of Schulz-distributed radii and the Zimm parameter, Z, defines the relative width, p, of the distribution: $p(\%) = 100/(Z+1)^{1/2}$.

The number of scatterers per unit volume, n_{sc}, is given as $(c-c_m)N_A/(M_n n_{ag})$, where c is the concentration of the solute, c_m is the critical concentration (both quoted in units of mass per volume), N_A is Avogadro's number, M_n is the solute molar mass and $n_{ag} \geq 1$ is the – unknown – aggregation number. The aggregation number in the expression for n_{sc} is eliminated by expressing it in terms of the mean volume of the scatterers and of the monomers as $n_{ag} = 4\pi\langle R^3\rangle/[3(v + n_s v_s)]$. c_m was determined at 25 °C by fluorescence spectroscopy using

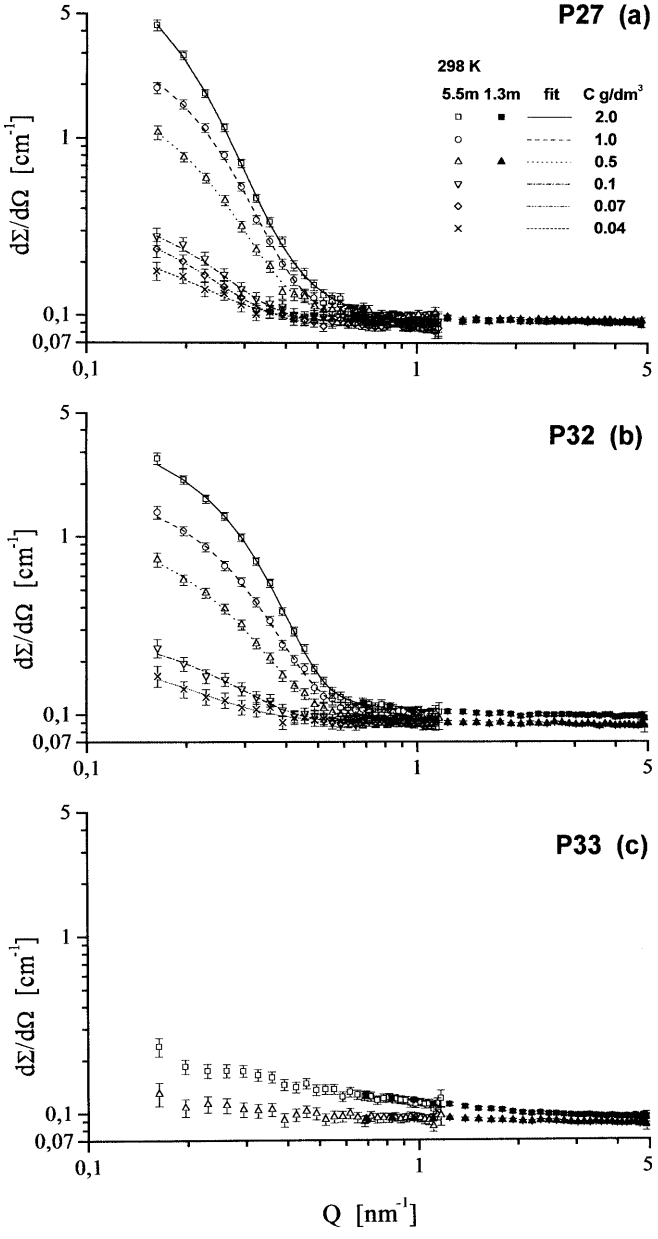

Fig. 1 Absolute small-angle neutron scattering (*SANS*) intensities obtained from different concentration solutions of **a** P27, **b** P32 and **c** P33 triblock copolymers. The *symbols* with error bars stand for raw data, the *lines* for best-fit curves from Eq. (2)

pyrene as a fluorescent probe [10]. Pyrene is strongly hydrophobic, and its solubility in water is extremely low. The method is based on the shift in the (0,0) band of the excitation spectra that is caused by the presence of a hydrophobic surrounding: $c_m \sim 0.003$–0.004 g/dm^3 was obtained for P27 and P32, and $c_m \sim 0.014$ g/dm^3 for P33 polymers [2].

Expressed with molecular parameters, the contrast of the scatterers is written in the form $\Delta\rho = n_{ag}(b - v\rho_s)/[n_{ag}(v + n_s v_s)] = (b - v\rho_s)/(v + n_s v_s)$. The quantities b and v, respectively, denote the scattering length and the volume of the polymer chains involved; ρ_s stands for solvent scattering length density, v_s for the volume of solvent molecules and n_s for the number of solvent molecules per monomer inside the aggregate. Finally, by considering that the mean value, $\langle R^3 \rangle$, of the Schulz-distributed quantity R equals $\bar{R}^3(Z+2)(Z+3)/(Z+1)^2$, and by introducing the variables $t = \lambda/\bar{\lambda}$ $u = R/\bar{R}$ and the notation $\eta = \bar{\lambda}/\Delta\lambda\sqrt{2}$, the model function is a number average of the elementary scattering intensities of the form

$$\frac{d\Sigma(Q)}{d\Omega} = A \int_0^\infty \frac{\eta}{\sqrt{\pi}} \exp\left[-\eta^2\left(\frac{1}{t} - 1\right)^2\right] \times \int_0^\infty \frac{3(Z+1)^2}{4\pi\bar{R}^3(Z+2)(Z+3)} F^2(tQ, u\bar{R}) \times u^Z \gamma(Z+1) \exp[-(Z+1)u] du \frac{dt}{t^2} + B \quad . \qquad (2)$$

The fitting parameters are $\bar{R}$ and Z, the correction constant, B, of incoherent scattering and the prefactor, A; this last quantity is related to the concentrations and the molecular parameters of the polymer chains by the following equation:

$$A = (c - c_m)\frac{N_A}{M_n}\frac{(b - v\rho_s)^2}{v + n_s v_s} = (c - c_m)S \quad . \qquad (3)$$

SANS patterns from P27 and P32 solutions could be successfully fitted by Eq. (2). The best-fit curves are plotted with solid lines in Fig. 1a and b; the best-fit values of $\bar{R}$ and Z are plotted versus solute concentration in Fig. 2, those of A are plotted in Fig. 3.

The mean radius, $\bar{R}$, of P32 type scatterers falls within 6–7 nm, that of P27-type ones within 8–9 nm and depends only slightly on the solute concentration. The values of the Schulz–Zimm parameter, Z, reflect the fact that the scatterers are polydisperse: p ~ 20–30%. For both the P27 and P32 solutions the best-fit values of A versus the solute concentration have the same straight line of slope $S = (8.33 \pm 0.39) \cdot 10^{20}$ g/cm. Since the ratio of the number of MMA to the number of NaA units in both polymers is the same (1:2), their scattering length is strictly proportional to the molar mass: $b = c_b M_n$, where c_b is a constant depending only on the composition of the polymer units. Because the slope was found to be the same for P27 and P32 polymers, v and n_s should depend on M_n in a way suitable to make the rational expression $S = N_A(c_b M_n - v\rho_s)^2/[M_n(v + n_s v_s)]$ independent of the type of polymer.

In the simplest and most reasonable cases one may assume that the molecular volume, v, of the polymer, like its scattering length, is also proportional to the molar mass, $v = c_v M_n$, resulting in $N_A M_n(c_b - c_v\rho_s)^2/(c_v M_n + n_s v_s)$ for S. S can be made independent of the type of polymer either if $n_s \sim c_n M_n$ or if $n_s v_s \ll v = c_v M_n$

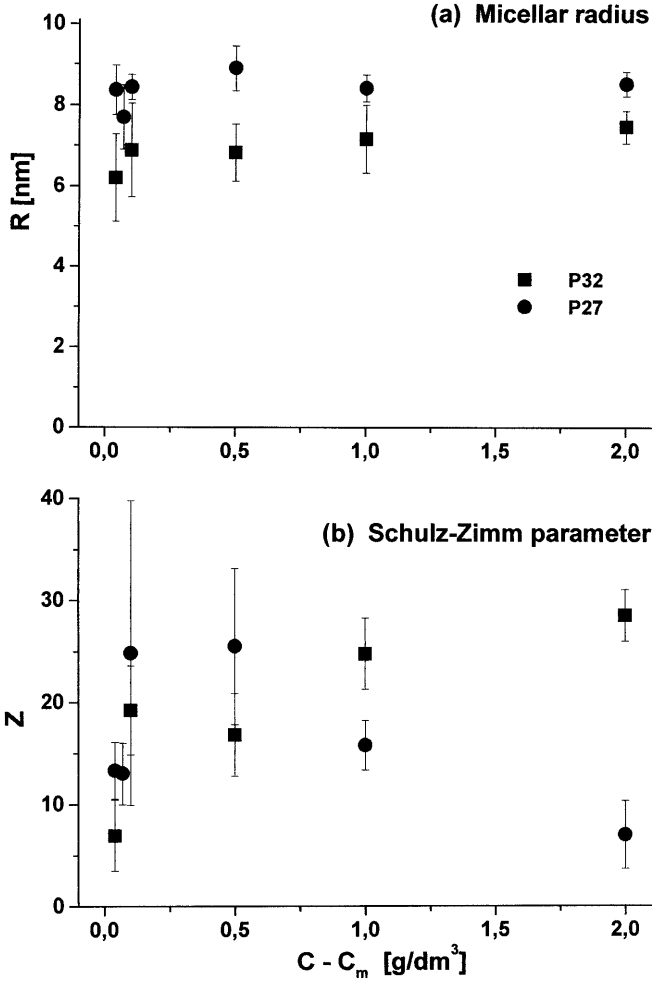

Fig. 2 **a** Micellar radius, $\bar{R}$ and **b** the Schulz–Zimm width parameter, Z, obtained by fitting Eq. (2) to SANS patterns from aqueous solutions of P27- and P32-type tribock copolymers, as a function of aggregated solute concentration

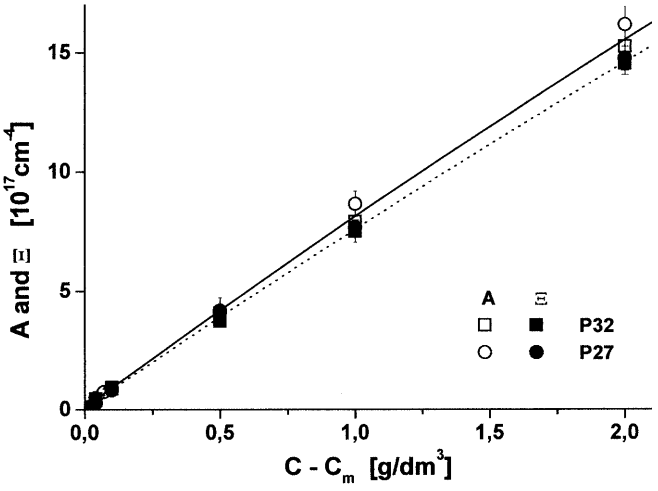

Fig. 3 Prefactor A obtained by fitting Eq. (2) to SANS patterns from aqueous solutions of P27- and P32-type tribock copolymers, and the Porod invariant, Ξ; both quantities as a function of aggregate solute concentration

holds. The first condition corresponds to the assumption that the number of solvent molecules per polymer chain, solubilized by the micelles, is proportional to the length of the hydrophobic blocks; the second expresses the strong hydrophobicity of the MMA units. Both conditions are realistic and both may hold at the same time. Provided that S and n_s are known, a quadratic equation can be derived for v. By introducing the notation $f = SM_n/(N_A\rho_s^2)$ and $v_{eq} = b/\rho_s$, we have $v^2 - v(f + 2v_{eq}) + v_{eq}^2 - fn_sv_s = 0$. Because of the strong hydrophobicity of the MMA units, n_s was set to 0 and the equation was solved assuming that the mean volume of the scatterers is filled either by the hydrophobic blocks only or by the entire polymer chains. Nuclear data were taken from Ref. [11] and solvent molecular volumes from Ref. [12]. The results summarized in Table 2 show that a realistic, ~1.1–1.2 g/cm^3, density inside the aggregates can be achieved if the observed scattering patterns are assumed to arise only from the hydrophobic blocks. In this case $n_{ag} \gg 1$, indicating that P27- and P32-type triblock copolymers aggregate in aqueous surroundings.

Although fluorescence spectroscopy indicates that aggregation also takes place in solutions of P33-type polymers, the scattering patterns from P33 solutions (Fig. 1c) could not be treated within the framework of this model. The hydrophobic blocks of P33-type polymers are probably short for forming compact micellar cores (the existence of a minimum chain length necessary for micelle formation is well known among ionic surfactants [13]). However, the formation of small loose aggregates, or unimolecular micelles, where the fluorescent dye tests hydrophobic surrounding, is still possible.

Let us consider now the Porod invariant, $\Xi = (1/2\pi^2)\int_0^\infty Q^2[d\Sigma(Q)/d\Omega]dQ$ [14]. It equals the spatial average, $\overline{\Delta\rho^2}$, of the squared scattering contrast, in dilute systems being expressed in terms of the volume fraction, ξ, and the scattering contrast of the individual micelles as $\overline{\Delta\rho^2} = \xi(\Delta\rho)^2$. The volume fraction of the micelles is defined as $\xi = (c - c_m)N_A\langle V\rangle/(M_n n_{ag})$, where $\langle V\rangle = 4\pi\langle R^3\rangle/3$ is the mean volume of the micelles. By considering that $\langle V\rangle/n_{ag} = v + n_s v_s$, the Porod invariant is defined by the same formula as the prefactor in Eq. (3). The experimental values obtained for Ξ are plotted in Fig. 3, along with the prefactor A. The comparison of the two data sets shows acceptable agreement. Though the invariant is slightly, but systematically, less than the prefactor, their difference (which may be caused by the truncation of the scattering patterns) is not significant and falls within the range of the experimental errors.

Table 2 Estimation of v, the molecular volume of the core-forming fraction of the polymer chain, d_{ag}, its density and n_{ag}, the aggregation number from scattering length, b, and parameter combinations f and v_{eq}; for the latter two see the text

Polymer	$b\times10^{10}$ (cm)	$f\times10^{21}$ (cm^3)	$v_{eq}\times10^{10}$ (cm^3)	$v\times10^{21}$ (cm^3)	d_{ag} (g/cm^3)	N_{ag}
P27	5.28	34.7	8.3	49.9	1.17[a]	46–74
	22.25	34.7	35.1	91.4	1.59[b]	
P32	1.94	12.9	3.06	18.5	1.13[a]	75–105
	8.17	12.9	12.9	33.8	1.61[b]	

[a] The aggregate is formed only by the hydrophobic blocks
[b] The aggregate is formed by the entire polymer chains

The scattering curves, $[d\Sigma(Q)/d\Omega - B]/(c - c_m)$, normalized to micelle-forming solute concentration are plotted for P32- and P27-type polymers in Fig. 4a and b, respectively. For a particular polymer the normalized intensities agree within experimental error, suggesting that in the applied concentration range c has no perceptible effect on the aggregation of a particular polymer chain. This property of the scattering curves and the linear dependence of A and Ξ on solute concentration confirm the conclusion that the hydration conditions inside the micellar cores of P27- and P32-type aggregates are similar, in spite of the fact that the normalized absolute intensity curves in Fig. 4a and b reflect structures of slightly different conformation.

Results at lower Q. Salt effects

Measurements in a range extended towards lower Q were performed in Jülich in 1, 5 and 10 g/dm^3 concentration solutions at 298 K, with and without 1 M added NaCl. The solutions were prepared from P32 (ABA-type) as well as from P8 (BAB-type) polymers. The scattering curves are plotted in Figs. 5 and 6, respectively. The scattering curves from solutions without electrolyte added resemble those from micellar solutions of low-molecular-weight ionic surfactants.

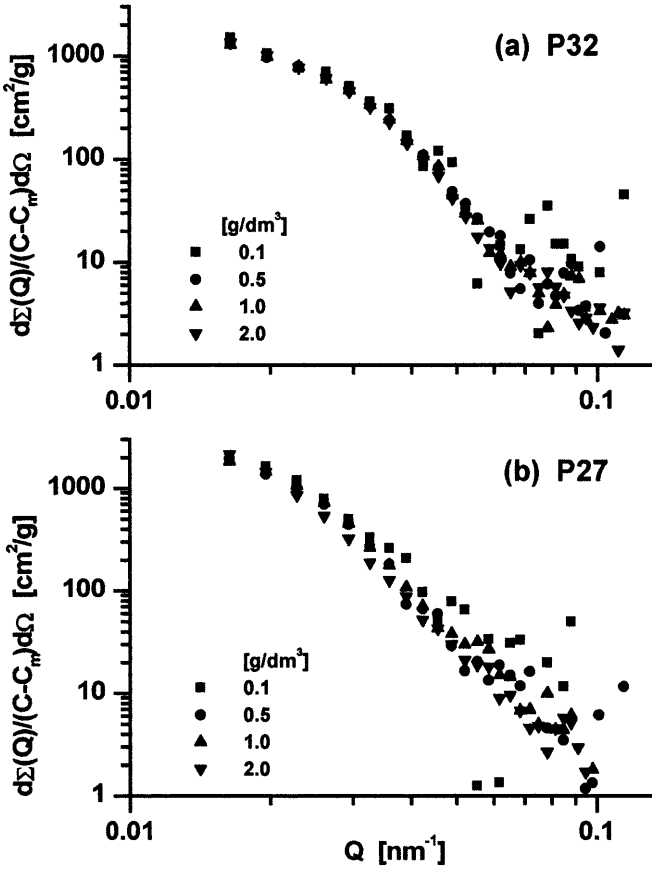

Fig. 4 Absolute SANS intensities from 0.1, 0.5, 1 and 2 g/dm^3 concentration solutions of **a** P32- and **b** P27-type triblock copolymers, normalized to solute concentration

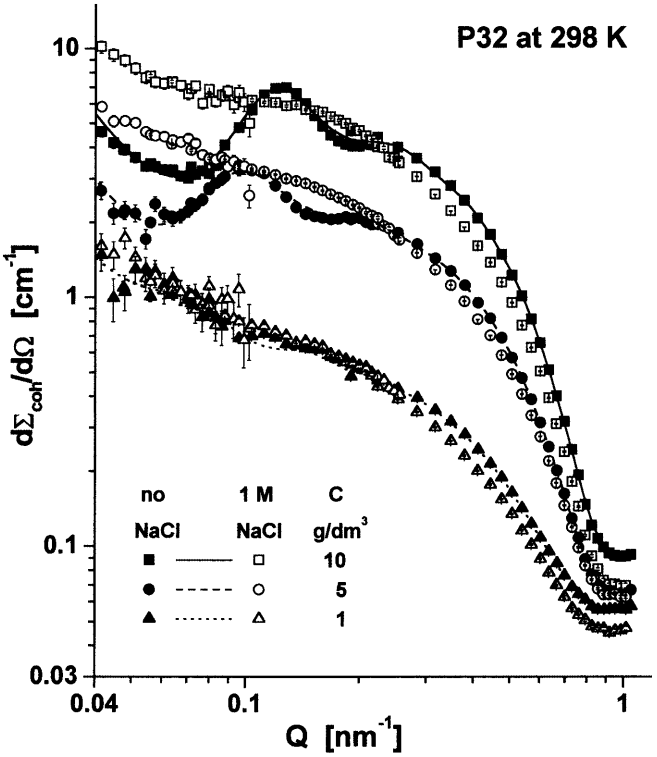

Fig. 5 Absolute SANS intensities obtained from 1, 5 and 10 g/dm^3 concentration solutions of P32-type triblock copolymers, with (*open symbols*) and without 1 m NaCl added (*filled symbols*)

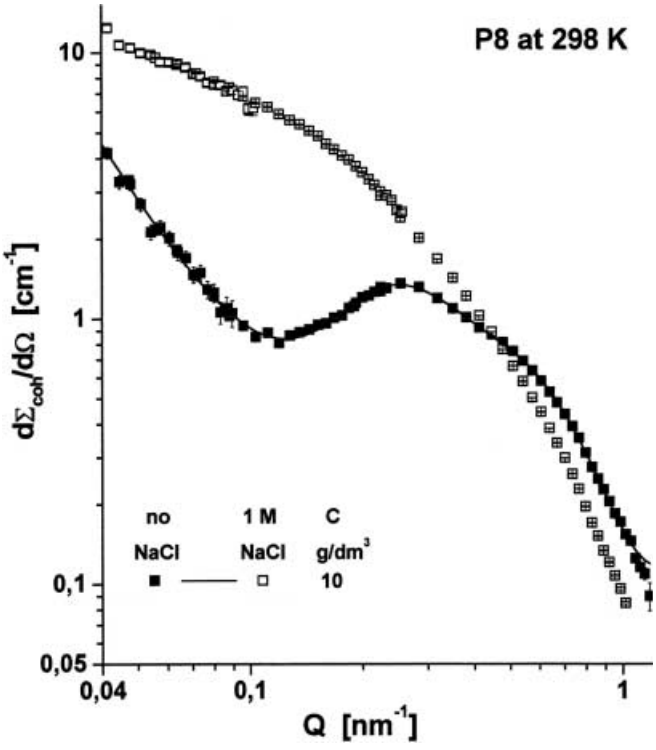

Fig. 6 Absolute SANS intensities obtained from 10 g/dm^3 concentration solutions of P8-type triblock copolymers, with (*open symbols*) and without 1 M NaCl added (*filled symbols*)

In analogy with ionic surfactant micelles, an attempt is made to describe the scattering curves from polydisperse copolymer micelles in terms of the elementary scattering amplitudes, $A_i(Q)$, of the micelles and of their partial structure factors, $S_{ij}(Q)$, by the formula

$$\frac{d\Sigma(Q)}{d\Omega} = n_{sc}\left[\sum_i W_i\langle A_i^2(Q)\rangle - \left(\sum_i W_i\langle A_i(Q)\rangle\right)^2 + \sum_i\sum_j W_iW_j\langle A_i(Q)\rangle\langle A_j(Q)\rangle S_{ij}(Q)\right] , \quad (4)$$

where the angled brackets denote thermodynamic averaging, and W_i is the probability of finding a micelle with aggregation number i [15]. From the agreement of the gyration and hydrodynamic radii of P32 micelles obtained from static and dynamic light scattering, respectively, Eq. (4) is simplified by assuming that the micelles are spherical [2]. In this case the first two terms on the right-hand side of Eq. (4), which stand in the general case for size and shape fluctuations, cancel. In order to avoid the lengthy numerical determination of the partial structure factors, the set of $S_{ij}(Q)$ is replaced by a mean structure factor $S(Q)$ [16], leading to the well-known approximate form

$$\frac{d\Sigma(Q)}{d\Omega} \approx n_{sc}P(Q)S(Q) , \quad (5)$$

where $P(Q)$ is the two-shell variant of Eq. (2). Provided that $P(Q)$ stands for a two-shell scatterer, the proper interpretation requires the knowledge of the scattering contrast (i.e. the molecular volume) of both types of chain and of the mean shell thickness.

In the previous paragraph the scattering patterns were assumed to arise mainly from a compact micellar core, and with this assumption a physically reasonable value was obtained for the molecular volume of the core-forming chains that corresponds to ~1.15 g/cm^3 bulk pMMA density (Table 1). The molecular volumes of the pNaA chains were calculated from the same hypothetical bulk density and the thickness of the shell was considered to be free fitting parameter.

The structure factor is the Fourier transform of the spatial pair–correlation function of the scatterers, determined from their interaction potential, $U(r)$. The interaction of charged copolymer micelles consists of volume exclusion and electrostatic components. The volume exclusion results in a hard-sphere radius, R_0, for which $U(r) = \infty$ if $r \le 2R_0$.

In this approach the micelles are represented by spherical electric double layers of inner radius R_0, immersed in a structureless medium of dielectric constant ε. The DLVO potential is derived by solving the linearized Poisson–Boltzmann equation under the condition that the electrostatic potential on the boundaries of both interacting particles has the same value, $\psi_0 = \psi(R_0)$. The only requirement for deriving the DLVO potential formula is that the dipole and quadrupole momenta of the field disappear on the particle boundaries [7], and this condition can be satisfied if the polyelectrolyte has spherical symmetry. For $r > 2R_0$ the DLVO potential is described by the approximate form

$$U(r) \approx \varepsilon R_0\psi_0^2\frac{\exp[-\kappa R_0(r/R_0 - 2)]}{r/R_0} , \quad (6)$$

where κ is the inverse Debye–Hückel screening length. Numerical calculation of the structure factor on the basis of the interaction potential (Eq. 6) was made by a frequently tested root-mean-squares analysis algorithm [17, 18].

The evaluation of the scattering patterns in terms of Eq. (5) leads to an acceptable fit for the scattering curves from solutions without NaCl added; the best-fit curves are also plotted in Figs. 5 and 6. Core radii, $\bar{R}$, aggregation numbers, n_{ag}, and the values of Q_m, the maximum location of the scattering curves, are listed in Table 3. The thickness of the shell was found to be about 25–30 nm, and, in contrast to our expectation, no significant difference was found between the ABA- and BAB-type polymers. The reason for this is probably the very poor approach presented by the two-shell model. By fixing ε at 79.6, the dielectric constant of bulk water,

Table 3 Results obtained versus solute concentration, c, from measurements at lower Q for the mean core radius, $\bar{R}$, the mean aggregation number, n_{ag}, the maximum location, Q_m, of the interaction peaks and the mean distance, D, of the micelles

Polymer	c (g/dm^3)	$\bar{R}$		n_{ag}	Q_m (/nm)	D (nm)	
		Eq. (2)	Eq. (5)			Eq. (7)	Eq. (8)
P8	10		3.5	6	0.250	31	29
P32	1	4.9	5.2	44	0.054	143	136
	5	5.0	5.4	40	0.096	80	79
	10	5.1	5.4	48	0.125	62	63

for the hard-sphere radius the fit resulted in $R_0 \sim 15 \pm 3{-}5$ nm, regardless of solute concentration and block sequence. The potential strength parameter, ψ_0, and the characteristic length, $1/\kappa$, of the electrostatic field both turned out to be poorly defined fitting parameters, the former being greater than about $50k_BT$, the latter varying in the range 20–40 nm.

Neutron scattering predicts somewhat larger particles than light scattering: the aggregation number from the latter is 20 ± 2, the hydrodynamic radius in the concentration range 0.4–0.6 g/dm^3 varies between about 23–27 nm [2]. Because the wavelength of neutrons varied in the range 0.5–0.7 nm and that of the photons was 514.5 and 647.1 nm, the interference of neutrons provides a much more reliable picture on the structure of micelles than that of light quanta.

In order to compare the methods used in interpreting the scattering patterns at higher and lower Q, the scattering curves from the newly prepared solutions were also evaluated in terms of the compact core model (Eq. 2) in the range $Q > 0.15$/nm. The core radii obtained from the test are also listed in Table 3 and the results from the two models agree within the experimental error of ± 0.3–0.5 nm. The best-fit values of A also determine a straight line, the slope of which differs by about 15% from that of the previously prepared polymers plotted in Fig. 3; this difference falls within the range of the systematic error of converting scattering curves into absolute units. The agreement implies that the newly prepared P32 polymers, probably owing to differences in the preparation, form somewhat smaller micelles than previously; however, their mean scattering properties remain unchanged.

A further test of Eq. (5) can be made by considering that the values of Q_m should define a straight line versus $c^{1/3}$. According to Ref. [19], in solutions of ionic micelles the product of Q_m and of the mean spacing, D, of the micelles was found to be constant,

$$Q_m D = 7.965 \ , \tag{7}$$

equivalent to $Q_m \sim 1/D \sim c^{1/3}$. In Fig. 7 the maximum locations of the structure factor derived from P32

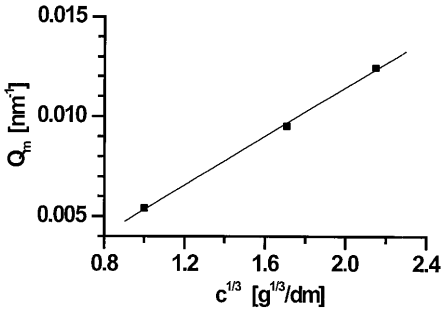

Fig. 7 Maximum location, Q_m, of the P32 scattering curves as a function of the cube root of the solute concentration

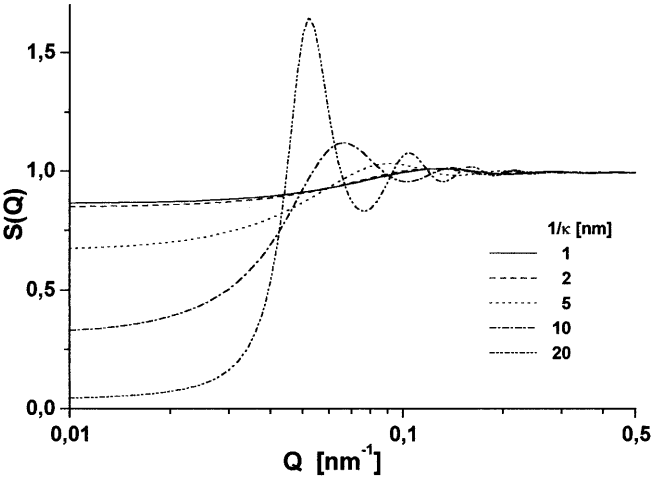

Fig. 8 Structure factor of hypothetical charged spheres by varying the screening length parameter

spectra define a straight line versus $c^{1/3}$; this finding supports the idea that the scatterers are individual entities rather than bound in a network by the hydrophilic blocks. D was calculated partly in a model-free way from Eq. (7), partly from Eq. (8) by making use of the mean aggregation numbers obtained from fitting Eq. (5) to scattering spectra:

$$D = \left(\frac{n_{ag} M_n}{N_A (c - c_m)} \right)^{1/3} \times 10^8 \text{ nm} \ . \tag{8}$$

The results from both equations are listed in Table 3; their agreement supports the validity of the structure factor calculations.

Scattering curves from solutions with added NaCl are also plotted in Figs. 5 and 6. At lower Q the scattering intensity significantly increases and the local maxima corresponding to the interaction peaks, found both in P32 and P8 systems without electrolyte added, disappear. The salt effect on the shape of the scattering curves can be understood from a qualitative analysis of $S(Q)$ in terms of the screening length as well as from the

Guinier approximation to $d\Sigma(Q)/d\Omega$. The presence of salt changes the value of $1/\kappa$, the Debye–Hückel screening length. In order to demonstrate the effect of salt on the shape of the scattering curves, the structure factor was calculated according to the method of Hayter and Pennfold [17, 18] for various values of $1/\kappa$ ranging from 1 to 20 nm. The results are plotted in Fig. 8: by decreasing the value of $1/\kappa$, the sharp $S(Q)$ function tends to become a flat curve and for $1/\kappa \leq 2$ nm no significant change can be observed in the $S(Q)$ curves. Since $1/\kappa$ in a 1 M NaCl solution is about 0.3 nm, the behavior of the $S(Q)$ curves in Fig. 8 explains why the interaction peaks disappear in the scattering patterns from salted solutions.

Provided that the radius of gyration, R_g, satisfies the condition $(R_gQ)^2 \ll 3$, the scattering intensity can be approximated by the Guinier formula as $d\Sigma(Q)/d\Omega \approx [d\Sigma(q)/d\Omega|_{Q=0}]\exp[-(R_gQ)^2/3]$. The salt screens the repulsion between the charged units and thus causes a collapse in the spatial arrangement of the hydrophilic chains, resulting in two consequences. First, the contrast distribution of the micelle compresses, resulting in a decrease in the radius of gyration: $R_g^s < R_g$, where the superscript s denotes quantities from salted systems. Therefore the scattering curves from salted systems are expected to exert a less steep decrease at low Q, as seen in Figs. 5 and 6. In the case of ABA micelles, where both ends of the hydrophilic blocks are connected to the core, the changes induced by salt effects in the Guinier region of the scattering curves are expected to be relatively less than in the case of BAB ones, where the hydrophilic blocks float freely. The scattering curves in Figs. 5 and 6 support this expectation. Second, owing to their collapse, some of the hydrophilic blocks may stick to the core increasing its radius: $\bar{R}^s \geq \bar{R}$. This increase should be reflected in the scattering curves by the shift of their tails towards $Q = 0$, as really observed in both cases. The tails of the scattering curves from pure and salted P32 solutions practically overlap ($\Delta Q/Q \approx \Delta\bar{R}/\bar{R} \leq 0.05$) and again the P8 curves reflect the more significant structural change ($\Delta Q/Q \approx \Delta\bar{R}/\bar{R} \sim 0.15$). The assumed structure of the P32 and P8 micelles in nonsalted and salted solutions is demonstrated in Fig. 9.

The salt tolerance of triblock copolymer micelles is much better than that of low-molecular-weight surfactant micelles. According to a dynamic light scattering study [20], in a 2 g/dm^3 sodium dodecyl sulfate (SDS) solution at 293 K the addition of 1 mol/dm^3 NaCl causes a relative change in the hydrodynamic radius of the micelles of $\Delta R_h/R_h \sim 8-10$. Similar trends have been found with SANS for the core radius of SDS [21] and of alkyl poly(oxyethylene sulfate) micelles [22, 23]. A very qualitative explanation for the good salt tolerance is the entanglement of the long hydrophobic chains which may prevent them from any structural reorganization, at least on the timescale of the observation.

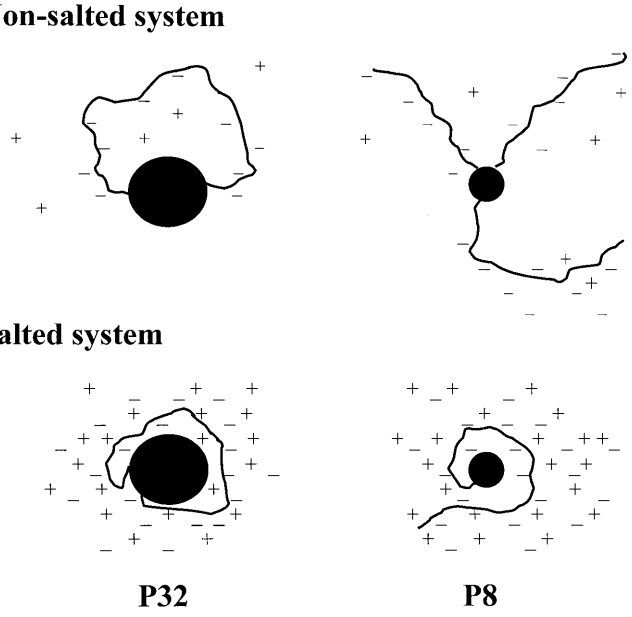

Fig. 9 Schematic picture of the arrangement of hydrophilic chains of P32- and P8-type triblock copolymer micelles in nonsalted and salted solutions. In nonsalted solutions the dissociated Na^+ ions cannot screen the negative charges bound to the hydrophilic chains, and the long-range Coulombic repulsion acting among the latter causes the hydrophilic chains to span the largest space possible. In salted solutions the charges are screened and the segments of the hydrophilic chains are separated mainly by short-range Lennard-Jones-type repulsion

Conclusions

Triblock copolymers built from pMMA and pNaA blocks aggregate into micelles in aqueous solution (probably if the length of the pMMA blocks exceeds a minimum length). The concentration dependence of the maximum location of the interaction peak suggests that the micelles form an interacting ensemble of individual particles rather than a network where the micelles are bound together by their pNaA blocks.

The compact core and the core–shell models applied to SANS spectra recorded at higher and lower Q, respectively, unequivocally support the idea that pMMA blocks form a compact micellar core. Although the models applied turned out to be unsuitable for determining the conformation of the pNaA blocks, from the extent of the collapse of the shell induced by added salt one can draw the conclusion that in ABA-type micelles the pNaA blocks are connected to the micellar cores by their both ends, in ABA type micelles only by one end. It should be pointed out, however, that without having either direct proof from a recent imaging technique such as cryogenic transmission electron miicroscopy or, at least, confirmation from a more detailed shell model, the present conclusions for the conformation of side chains in ABA- and BAB-type micelles cannot be considered unique.

From the concentration dependence of the Porod invariant one may conclude that the hydration of different ABA-type triblock copolymers (which consist of MMA and NaA units in the same proportion) depends neither on solute concentration nor on polymer chain length. The dilution and salt tolerance of these micelles is in agreement with the high (about 400 K) glass-transition temperature of the pMMA blocks [2, 24, 25].

Intermicellar interactions can be characterized empirically by a hard-sphere plus a DLVO potential. The fit results in reasonable values for the hard-sphere radius; however, the proper interpretation of the parameters of the DLVO potential requires further work. Model calculations explain how the added salt screens the interaction peak in salted solutions.

Acknowledgements Support from the Bundesministerium für Bildung und Forschung, BASF AG, Ludwigshafen, and the National Foundation for Scientific Research, Hungary, (OTKA) contract no. T029958 is gratefully acknowledged.

References

1. Klapper M, Haimer K (1999) Polym Mater Sci Eng 81:234
2. Haimer K (1999) PhD thesis. Gutenberg University, Mainz
3. Rodrigues K, Mattice WI (1992) Langmuir 8:456
4. Förster S, Hermsdorf N, Leube W, Schnabblegger H, Regenbrecht M, Akari S (1999) J Phys Chem B 103:6657
5. Raspaud E, Lairez D, Adam M, Carton J-P (1994) Macromolecules 27:2956
6. Raspaud E, Lairez D, Adam M, Carton J-P (1996) Macromolecules 29:1269
7. Verwey EJW, Overbeek JTG (1948) Theory of the stability of lyophobic colloids. Elsevier, New York
8. Grosius P, Gallot Y, Skoulios A (1970) Makromol Chem 35:35
9. Ishizu K, Kashi Y, Fukutomi T, Kakurai T (1982) Makromol Chem 183:3099
10. Zana R (1986) In: Zana R (ed) Surfactant Solutions: new methods of investigation. Dekker, New York, pp 241–294
11. Sears VF (1984) Thermal neutron scattering lengths and cross sections for condensed matter research. Report AECL-8940, Chalk River
12. Kell GSJ (1977) Chem Phys Ref Data 6:1109
13. Hiemenz PC (1986) Principles of colloid and surface chemistry. Dekker, New York
14. Porod G (1982) In: Glatter O, Kratky O (eds) Small-angle X-ray scattering. Academic, New York, pp 17–52
15. Vass S, Gilányi T, Borbély S (2000) J Phys Chem B 104:2073
16. Chen HS (1986) Physica B 137:183
17. Hayter JB, Penfold J (1980) SQHP: a FORTRAN package to calculate $S(Q)$ for macroion solutions. ILL report 80HA07S. ILL, Grenoble
18. Hayter JB, Penfold J (1982) The structure factor of charged colloidal dispersions at any density. ILL report 82HA14T. ILL, Grenoble
19. Chen SH, Sheu EY, Kalus J, Hoffmann HJ (1988) Appl Crystallogr 21:751
20. Missel PJ, Mazer NA, Benedek GB, Carey MC (1983) J Phys Chem 87:1264
21. Hayter JB, Penfold J (1983) Colloid Polym Sci 261:1022
22. Triolo R, Caponetti EJ (1986) Solution Chem 15:377
23. Caponetti E, Triolo R, Johnson JSJ Jr (1987) Solution Chem 16:295
24. Ferry JD (1980) Viscoelastic properties of polymers. Wiley, New York
25. Brandrup J, Immergut EP (1989) Polymer handbook. Wiley, New York